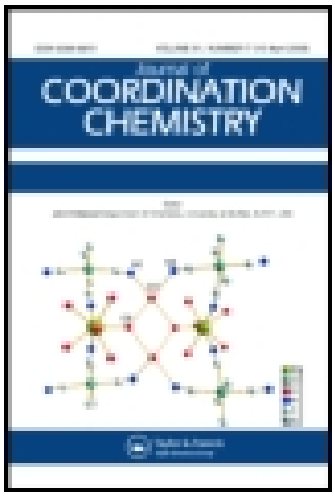

Journal of Coordination Chemistry
Publication details, including instructions for authors and subscription information:
http://www.tandfonline.com/loi/gcoo20

Crystal structures, spectroscopic, electrochemical and antibacterial properties of a series of new copper(II) Schiff base complexes

Nasibeh Imani[a], Mahdi Behzad[a], Hadi Amiri Rudbari[b], Giuseppe Bruno[c], Hamideh Samari Jahromi[d] & Ali Khaleghian[e]

[a] Department of Chemistry, Semnan University, Semnan 35351-19111, Iran

[b] Faculty of Chemistry, University of Isfahan, Isfahan 81746-73441, Iran

[c] Università degli Studi di Messina, dip. Scienze Chimiche. Viale Ferdinando S. d'Alcontres, 98166 Messina, Italy

[d] Research Institute of Petroleum Industry (RIPI), Environment and Biotechnology Division, West Blvd., Azadi Sports Complex, P.O. Box 14665-1998, Tehran, Iran

[e] Semnan University of Medical Science, Faculty of Medicine, Biochemistry Department, Semnan, Iran

Accepted author version posted online: 20 May 2015.

To cite this article: Nasibeh Imani, Mahdi Behzad, Hadi Amiri Rudbari, Giuseppe Bruno, Hamideh Samari Jahromi & Ali Khaleghian (2015): Crystal structures, spectroscopic, electrochemical and antibacterial properties of a series of new copper(II) Schiff base complexes, Journal of Coordination Chemistry, DOI: 10.1080/00958972.2015.1051476

To link to this article: http://dx.doi.org/10.1080/00958972.2015.1051476

Publisher: Taylor & Francis
Journal: *Journal of Coordination Chemistry*
DOI: http://dx.doi.org/10.1080/00958972.2015.1051476

Crystal structures, spectroscopic, electrochemical and antibacterial properties of a series of new copper(II) Schiff base complexes

NASIBEH IMANI[a], MAHDI BEHZAD*[a], HADI AMIRI RUDBARI[b], GIUSEPPE BRUNO[c], HAMIDEH SAMARI JAHROMI[d] and ALI KHALEGHIAN[e]

[a]Department of Chemistry, Semnan University, Semnan 35351-19111, Iran
[b]Faculty of Chemistry, University of Isfahan, Isfahan 81746-73441, Iran
[c]Università degli Studi di Messina, dip. Scienze Chimiche. Viale Ferdinando S. d'Alcontres, 98166 Messina, Italy
[d]Research Institute of Petroleum Industry (RIPI), Environment and Biotechnology Division, West Blvd., Azadi Sports Complex, P.O. Box 14665-1998, Tehran, Iran
[e]Semnan University of Medical Science, Faculty of Medicine, Biochemistry Department, Semnan, Iran

Two new and two previously reported Schiff base ligands as well as four corresponding new Cu(II) complexes (CuL^{1-4}) were synthesized and characterized. The Schiff base ligands were synthesized from condensation of 5-bromo-2-hydroxy-3-nitrobenzaldehyde with aliphatic (H_2L^{1-2}) or aromatic (H_2L^{3-4}) diamines. Crystal structures of CuL^2 and CuL^3 were determined by X-ray crystallography. Antibacterial properties of these ligands and complexes were studied against four human pathogenic bacteria. The complexes showed moderate antibacterial activities, higher than those of the ligands.

Keywords: Schiff base; Copper(II); Crystal structure; Antibacterial activity

1. Introduction

Transition metal complexes of Schiff base ligands have attracted interest due to their potential applications in dye and food industries, catalysis and biochemistry [1-10]. This is mainly due to the fact that such ligands could be easily synthesized and the electronic and/or steric properties of their complexes could be finely tuned by introducing different substituents on both the diamine and the aldehyde/ketone moieties. Furthermore, Schiff base ligands usually make stable complexes with a large number of d- and f-block metal ions, providing the possibility to study different aspects of such complexes. From the biological standpoint, Schiff base complexes have

*Corresponding author. Emails: mbehzad@semnan.ac.ir; mahdibehzad@yahoo.com

been used as models of biological compounds and have been key in the development of inorganic biochemistry [11]. Having all the above facts in mind, we focused on the synthesis and study of antibacterial activities of a series of transition metal Schiff base complexes [12-15]. In our previous studies, we found that the presence of more electronegative substituents on the salicylaldehyde moieties of the Schiff base ligands increased the antibacterial activity of their complexes. Therefore, we decided to synthesize new copper(II) complexes of a series of electronegativity enhanced Schiff base ligands derived from condensation of different aliphatic and aromatic diamines with 5-bromo-2-hydroxy-3-nitrobenzaldehyde. The antibacterial activities of the ligands and the corresponding Cu(II) complexes were studied against two Gram-positive and two Gram-negative human pathogenic bacteria; *Escherichia Coli* (Gram-negative), *Salmonella typhi* (Gram-negative), *Staphylococcus aureus* (Gram-positive) and *Bacillus subtilis* (Gram-positive). Our results showed that these Cu(II) complexes had moderate antibacterial activities and their activities were higher than those of their corresponding ligands.

2. Experimental

2.1. *Materials and methods*

All chemicals and solvents were purchased from commercial sources and used as received. 5-Bromo-2-hydroxy-3-nitrobenzaldehyde [16], H_2L^1 and H_2L^3 [17, 18] were synthesized as described elsewhere. Melting points were obtained on a thermoscientific 9100 apparatus. Elemental analyses were performed on a Perkin-Elmer 2400II CHNS-O analyzer. ^{1}H NMR spectra were recorded on a 500 MHz Bruker FT-NMR spectrometer using DMSO-d^6 as solvent; chemical shifts (δ) are given in ppm. IR spectra were obtained as KBr plates using a Tensor 27 Bruker FT-IR instrument. UV-Vis spectra were obtained on a Shimadzu UV-1650PC spectrophotometer. A Metrohm 757 VA computrace instrument was employed to obtain cyclic voltammograms.

2.2. *Synthesis of the Schiff bases*

2.2.1. Synthesis of H_2L^2. Schematic representation of the synthesis procedures is shown in scheme 1. For this ligand, to a vigorously stirred and boiling solution of 5-bromo-2-hydroxy-3-nitrobenzaldehyde (0.25 g, 1 mmol) in 15 mL methanol was added a solution of 0.52 g (0.5 mmol) 2,2-dimethyl-1,3-propanediamine in 15 mL methanol. The reaction mixture was

refluxed for 3 h while the progress of the reaction was monitored by TLC. The solid orange product was collected by filtration, washed with 10 mL of boiling methanol and air dried to yield 0.43 g of the target ligand (78%). M.P. = 216-7 °C. Selected IR (cm^{-1}): 3467, 1647, 1508. ^{1}H NMR (DMSO-d^6): 14.82 (2H, br), 8.66 (2H, s), 8.12 (2H, d), 7.82 (2H, d), 3.64 (4H, s), 1.03 (6H, s). UV-Vis. 10^{-5} M solution in DMF [λ_{max} nm, (ε $M^{-1}cm^{-1}$)]: 267 (14300), 471 (15500). Anal. Calcd. for $C_{19}H_{18}Br_2N_4O_6$: C, 40.88; H, 3.25; N, 10.04. Found: C, 40.79; H, 3.20; N, 10.10.

2.2.2. Synthesis of H_2L^4. This ligand was prepared similar to H_2L^2 except 4-methyl-1,2-phenylenediamine was used instead of 2,2-dimethyl-1,3-propanediamine. Yield was 0.44 g (67%). Selected IR (cm^{-1}): 3440, 1627, 1500. ^{1}H NMR (DMSO-d^6): 8.49 (1H, s), 8.17 (1H, s), 8.02-7.15 (7H, m), 5.46 (3H, s). UV-Vis. 10^{-4} M solution in DMF [λ_{max} nm, (ε $M^{-1}cm^{-1}$)]: 264 (16800), 329 (4800), 438 (17000). Anal. Calcd. for $C_{21}H_{14}Br_2N_4O_6$: C, 43.63; H, 2.44; N, 9.69. Found: C, 43.58; H, 2.38; N, 9.75.

2.3. ***Synthesis of the complexes***

2.3.1. Synthesis of CuL^1. 1 mmol (0.52 g) of H_2L^1 was dissolved in 10 mL methanol and was heated to reflux. To this solution was added a methanolic solution of 1 mmol of $Cu(OAc)_2$ (0.2 g in 10 mL). The reaction mixture was refluxed for 4 h. The brown solid product was collected by filtration and washed with 15 mL of hot methanol and air dried. Recrystallization from DMSO yielded 0.51 g (89%) of the target complex in three weeks. Selected IR (cm^{-1}): 1647, 1506. UV-Vis. 10^{-5} M solution in DMF [λ_{max} nm, (ε $M^{-1}cm^{-1}$)]: 265 (17800), 400 (7400), 620 (77). Anal. Calcd. for $C_{16}H_{10}Br_2CuN_4O_6$: C, 28.05; H, 1.73; N, 9.70. Found: C, 28.11; H, 1.68; N, 9.75.

2.3.2. Synthesis of CuL^2. This complex was prepared following similar procedure as described for CuL^1 except H_2L^2 was used instead of H_2L^1. Ether diffusion to an ethanolic solution of the complex yielded 0.56 g (90%) of the target complex in one week. Selected IR (cm^{-1}): 1633, 1508. UV-Vis. 10^{-5} M solution in DMF [λ_{max} nm, (ε $M^{-1}cm^{-1}$)]: 265 (29600), 421 (7100), 614 (175). Anal. Calcd. for $C_{19}H_{16}Br_2CuN_4O_6$: C, 36.80; H, 2.58; N, 9.04. Found: C, 36.72; H, 2.62; N, 9.11.

2.3.3. Synthesis of $CuL^3.2DMF$. This complex was prepared following similar procedure as described for CuL^1 except H_2L^3 was used instead of H_2L^1. Ether diffusion to a DMF solution of the complex yielded 0.48 g (62%) of the target complex in one week. Selected IR (cm^{-1}): 1616, 1500. UV-Vis. 10^{-5} M solution in DMF [λ_{max} nm, (ε $M^{-1}cm^{-1}$)]: 269 (27500), 312 (19900), 435 (18800), 598 (238). Anal. Calcd. for $C_{26}H_{24}Br_2CuN_6O_8$: C, 40.42; H, 3.11; N, 10.88. Found: C, 40.44; H, 3.17; N, 10.80.

2.3.4. Synthesis of CuL^4. This complex was also prepared following similar procedure as described for CuL^1 except H_2L^4 was used instead of H_2L^1. Ether diffusion to a DMF solution of the complex yielded 0.50 g (78%) of the target complex in one week. Selected IR (cm^{-1}): 1618, 1502. UV-Vis. 10^{-4} M solution in DMF [λ_{max} nm, (ε $M^{-1}cm^{-1}$)]: 267 (29700) 329 (12800) 432 (18800), 598 (234). Anal. Calcd. for $C_{20}H_{10}Br_2CuN_4O_6$: C, 38.36; H, 1.60; N, 8.95. Found: C, 38.44; H, 1.67; N, 8.90.

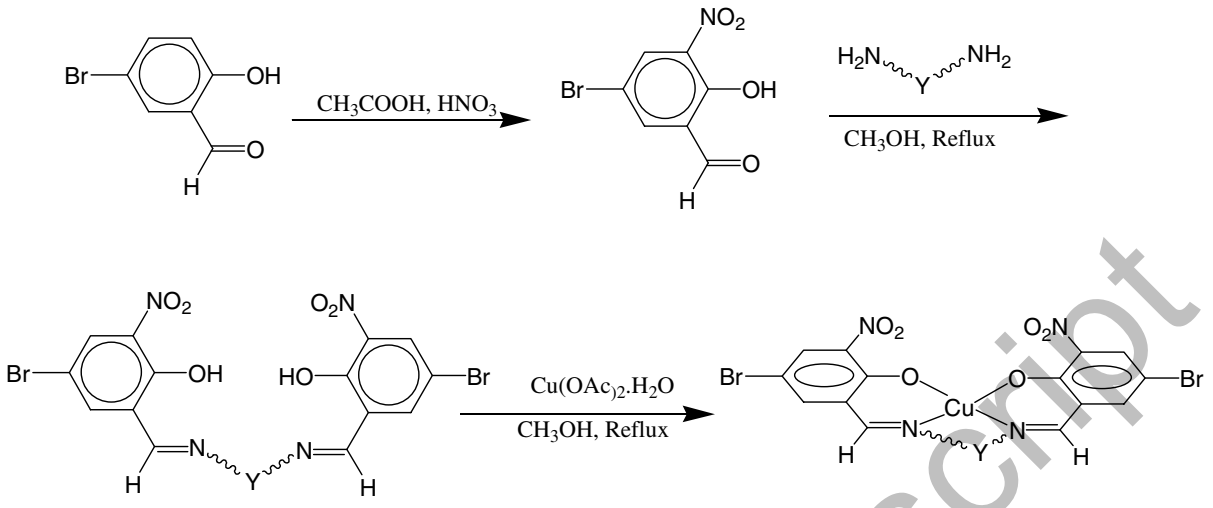

Ligand	Complex	Y
H_2L^1	CuL^1	
H_2L^2	CuL^2	
H_2L^3	CuL^3	
H_2L^4	CuL^4	

Scheme 1. Syntheses procedures.

2.4. *X-ray crystallography*

For CuL^2, data were collected at room temperature with a Bruker APEX II CCD area-detector diffractometer using MoKα radiation (λ = 0.71073 Å). Data collection, cell refinement, data reduction and absorption correction were performed using multiscan methods with Bruker software [19]. The X-ray diffraction measurement for CuL^3 was made on a STOE IPDSII diffractometer with graphite monochromated MoKα radiation. Data were collected at 293(2) K in a series of ω scans in 1° oscillations and integrated using the Stoe X-AREA software package [20]. A numerical absorption correction was applied using PLATON software [21]. The data were corrected for Lorentz and polarizing effects. Both structures were solved by direct methods

using SIR2004 [22]. The non-hydrogen atoms were refined anisotropically by the full matrix least squares method on F^2 using SHELXL [23]. All hydrogens (H) were placed at calculated positions and constrained to ride on their parent atoms. Details concerning collection and analysis for both complexes are reported in table 1.

2.5. *Electrochemical studies*

Electrochemical behavior of the complexes was studied by cyclic voltammetry in the potential range of 0 to -2.0 volts. DMSO was used as solvent and 0.1 M tetra-n-octylammonium bromide (TOAB) as supporting electrolyte. The experiments were conducted at room temperature under N_2 using a glassy carbon working electrode, a platinum auxiliary electrode and a Ag/AgCl reference electrode. The electrochemical data for the complexes are collected in table 3 and are corrected against $Fc^{+/0}$.

2.6. *Antibacterial studies*

2.6.1. Bacterial strains. The metal complexes were tested against *Salmonella typhi* (ATCC 19430), *Escherichia Coli* (ATCC 25922), *Staphylococcus aureus* (ATCC 25923) and *Bacillus subtilis* (ATCC 6633).

2.6.2. Determination of minimum inhibitory concentrations (MIC) and minimal bactericidal concentrations (MBC). Minimum inhibitory concentrations (MICs, μg mL^{-1}) were determined by the broth micro-dilution method following the procedures recommended by the National Committee for Clinical Laboratory Standards [24, 25]. MICs were defined as the lowest concentrations of compounds which inhibit the growth of microorganisms. All tests were performed in triplicate. Minimal bactericidal concentrations (MBCs) were also measured following a standard procedure [26]. 100 μL volumes of all clear (no growth) tubes from a dilution MIC test were spread on separate agar plates and incubated at 37 °C for 24 h. The MBC (μg mL^{-1}) was defined as the lowest concentration of the complex where no growth occurred.

3. Results and discussion

3.1. *Spectroscopic characterization of the ligands and complexes*

In the ^{1}H NMR of H_2L^2, the presence of a broad band above 12 ppm was assigned to the presence of phenolic protons. This signal was not observed for H_2L^4. This observation has been previously attributed to the rapid exchange in solution [16, 17]. The signals due to the iminic protons were observed at 8.66 for symmetric H_2L^2, and at 8.49 and 8.17 ppm for the unsymmetric H_2L^4. Other signals at 7-8.1 ppm were assigned to aromatic protons. The signals below 6 ppm were also assigned to aliphatic protons with appropriate peak area and were in agreement with the expected values [16, 17]. NMR spectra of the ligands are provided in figures S1 and S2. The most characteristic feature in the IR spectra of the Schiff base ligands and their metal complexes comes from the C=N stretching vibrations. In IR spectra of our ligands, these stretching vibrations are at 1640 cm^{-1} confirming the presence of the imine groups. These signals shifted to lower wavenumbers in the complexes which confirmed the coordination of Cu(II) to the iminic nitrogens. The presence of broad bands above 3400 cm^{-1} in IR spectra of the ligands was attributed to O-H stretching vibrations. These signals were eliminated from IR spectra of the complexes which confirmed the loss of the phenolic protons and the L^{2-} nature of the ligands in these complexes. The signals at 1500 cm^{-1} were also assigned to the NO_2 unsymmetrical stretches [27-29]. Electronic spectra of the ligands from the aliphatic amines, *i.e.* H_2L^1 and H_2L^2, showed two intense bands at 270 and 490 nm, assigned to the $\pi\rightarrow\pi^*$ and $n\rightarrow\pi^*$ transitions. UV-Vis spectra of H_2L^3 and H_2L^4 with aromatic amine moieties showed signals in similar regions as well as new intense bands at 300 nm. These new bands could be attributed to $\pi\rightarrow\pi^*$ transitions mostly centered on the new aromatic groups. In electronic spectra of CuL complexes, the above mentioned $\pi\rightarrow\pi^*$ signals were present in almost the same area but signals due to the $n\rightarrow\pi^*$ transitions disappeared; new signals at 420±20 and 610±20 nm have been observed. The former intense band could be attributed to the MLCT transitions while the latter weak bands were due to d-d transitions. These spectroscopic data are in agreement with previously reported similar complexes [27].

3.2. *X-ray crystallography*

3.2.1. Description of the crystal structure of CuL^2. Dark green crystals were obtained by slow evaporation of CH_3Cl solution of CuL^2 after one week. A suitable crystal with dimensions 0.15×0.21×0.30 mm was chosen for X-ray crystallography. Figure 1 shows an ORTEP representation of CuL^2 with atom numbering scheme. A summary of the crystallographic data,

and selected bond lengths and angles are collected in tables 1 and 2, respectively. The neutral species contains one Cu(II) coordinated to a doubly deprotonated ligand $(L^2)^{2-}$. All interatomic distances can be considered as normal and are in the common range of previously observed similar complexes [30, 31]. The geometry around the metal center is distorted square planar from the data collected in table 2. The angle between the planes defined by the two NCCCO chelating rings which is 30.23° confirms the distortion. No important hydrogen bond or π-π stacking was observed for CuL^2.

3.2.2. Description of the crystal structure of CuL^3. Dark green crystals of CuL^3 were obtained by ether diffusion into a DMF solution of the complex in a month. A suitable crystal with dimensions 0.18×0.25×0.33 was chosen for X-ray crystallography. An ORTEP drawing of this complex is shown in figure 2. The crystallographic data and selected bond lengths and angles are collected in tables 1 and 2, respectively. The metal ion is coordinated to $(L^3)^{2-}$ similar to CuL^2; however, the angle between the two NCCCO chelating ring systems in this complex is only 5.21° which indicates a very slightly distorted square planar arrangement around the metal center. The oxygen of one DMF of crystallization is located at 2.711(2) Å to the central metal ion. This interatomic distance is too long to be considered as a Cu-O bond, but might be responsible for the more flattened geometry of the Schiff base ligand. The average Cu-O (1.918 Å) and Cu-N (1.955 Å) bond distances are in the common range of similar complexes [30, 31].

3.3. *Electrochemistry*

Table 3 collects the results of the cyclic voltammetry studies and an illustrative example is shown in figure 3 for CuL^2. The complexes showed one quasi-reversible reduction wave at negative potentials corresponding to $Cu^{II/I}$ redox. Comparison of the E^0 values showed that the complexes with aromatic diamines were reduced in more negative values. The data were in the common range for previously studied similar complexes [30-32].

3.4. *Antibacterial studies*

The study of the antibacterial properties of Schiff bases and their metal complexes has attracted interest [33-39]. In our previous studies on the biological activities of the transition metal Schiff

base complexes, we found that the presence of more electronegative substituents on the ancillary ligand increased the antibacterial activity of their corresponding complexes. Similar results have also been reported by other researchers [33, 34]. Hence, we synthesized a series of Schiff base ligands with more electronegative substituents. The Schiff base ligands were synthesized from condensation of 5-bromo-2-hydroxy-3-nitrobenzaldehde with different aliphatic and aromatic diamines. The MIC and MBC values for the studied complexes against two Gram(+) and two Gram(-) human pathogenic bacteria are collected in table 4. The ligands did not show significant antibacterial activity but the complexes were moderately active against both Gram type bacteria. The increased activity of the complexes compared to the ligands could be explained by Overtone's concept [40] and Tweedy's theory [41]. The order of the antibacterial activity of the complexes is CuL^2>CuL^1>CuL^3>CuL^4. In this series, complexes with aliphatic amine moieties were more potent antibacterial agents than the corresponding aromatic analogues. A comparison with the electrochemical data which is CuL^2>CuL^1≈CuL^3>CuL^4 is also interesting. Although it is too soon to make complete conclusions, this could mean that electronic properties may play key roles in the designation of such antibacterial agents.

4. Conclusion

A series of Schiff base ligands derived from electronegative salicylaldehyde derivatives were synthesized. Their corresponding Cu(II) complexes were also synthesized. Crystal structure analyses showed that the geometry around the metal center was distorted square planar. Antibacterial studies showed that these complexes had moderate activity against both gram type bacteria. A correlation with the electrochemical data was also observed.

Appendix A. Supplementary material

CCDC 1005111 and 1048194 contains the supplementary crystallographic data for CuL^2 and CuL^3, respectively. These data can be obtained free of charge from the Cambridge Crystallographic Data Centre via www.ccdc.cam.ac.uk/data_request/cif.

References

[1] M.R. Maurya. *Coord. Chem. Rev.*, **237**, 163 (2003).

[2] C.R. Nayar, R. Ravikumar. *J. Coord. Chem.*, **67**, 1 (2014).

[3] D. Krajčiová, M. Melník, E. Havránek, A. Forgácsová, P. Mikuš. *J. Coord. Chem.*, **67**, 1493 (2014).

[4] S.Y. Ebrahimipour, M. Mohamadi, J. Castro, N. Mollania, H. Amiri Rudbari, A. Saccá. *J. Coord. Chem.*, **68**, 632 (2015).

[5] M. Amirnasr, R. Sadeghi Erami, K. Mereiter, K. Schenk, S. Meghdadi, S. Abbasi. *J. Coord. Chem.*, **68**, 616 (2015).

[6] W.-M. Zhang, M.-H. Li, J. Sun, P.-C. Lv, H.-L. Zhu. *J. Coord. Chem.*, **67**, 3519 (2014).

[7] M. Layek, M. Ghosh, M. Fleck, R. Saha, D. Bandyopadhyay. *J. Coord. Chem.*, **67**, 3371 (2014).

[8] L. Li, Z. Li, K. Wang, S. Zhao, J. Feng, J. Li, P. Yang, Y. Liu, L. Wang, Y. Li, H. Shang, Q. Wang. *J. Agric. Food Chem.*, **62**, 11080 (2014).

[9] Y. Jia, J. Li. *Chem. Rev.* (2014) Doi: 10.1021/cr400559g.

[10] A.W. Jeevadason, K.K. Murugavel, M.A. Neelakantan. *Renew. Sustain. Energy Rev.*, **36**, 220 (2014).

[11] A. Prakash, D. Adhikari. *Int. J. Chem. Tech. Res.*, **3**, 1891 (2011).

[12] A. Ghaffari, M. Behzad, G. Dutkiewicz, M. Kubicki, M. Salehi. *J. Coord. Chem.*, **65**, 840 (2012).

[13] H. Iranmanesh, M. Behzad, G. Bruno, H. Amiri Rudbari, H. Nazari, A. Mohammadi, O. Taheri. *Inorg. Chim. Acta*, **395**, 81 (2013).

[14] O. Taheri, M. Behzad, A. Ghaffari, M. Kubicki, G. Dutkiewicz, A. Bezaatpour, H. Nazari, A. Khaleghian, A. Mohammadi, M. Salehi. *Transition Met. Chem.*, **39**, 253 (2014).

[15] M. Salehi, M. Kubicki, G. Dutkiewicz, A. Rezaei, M. Behzad, S. Etminani. *Russ. J. Inorg. Chem.*, **39**, 716 (2013).

[16] A. Bezaatpour, M. Behzad, D.M. Boghaei. *J. Coord. Chem.*, **62**, 1127 (2009).

[17] D.M. Boghaei, A. Bezaatpour, M. Behzad. *J. Coord. Chem.*, **60**, 973 (2007).

[18] D.M. Boghaei, A. Bezaatpour, M. Behzad. *J. Mol. Catal. A*, **245**, 12 (2006).

[19] (a) COSMO, Version 1.60, Bruker AXS Inc., Madison, Wisconsin (2005). (b) SAINT, Version 7.06A, Bruker AXS Inc., Madison, Wisconsin (2005). (c) SADABS, Version 2.10, Bruker AXS Inc., Madison, Wisconsin (2005).

[20] Stoe, Cie, Program for the Acquisition and Analysis of Data X-AREA, Version 1.30, Stoe & Cie GmbH, Darmstadt, Germany (2005).

[21] A.L. Spek, PLATON, a multipurpose crystallographic tool, University of Utrecht: Utrecht, The Netherlands (1998).

[22] M.C. Burla, R. Caliandro, M. Camalli, B. Carrozzini, G.L. Cascarano, L. De Caro, Giacovazzo, C.G. Polidori, R. Spagna. *J. Appl. Crystallogr.*, **38**, 381 (2005).

[23] G.M. Sheldrick, SHELXL97, University of Göttingen, Göttingen, Germany (1997).

[24] Clinical and Laboratory Standards Institute. Performance Standards for Antimicrobial Susceptibility Testing: Nineteenth Informational Supplement M100–S19. Clinical and Laboratory Standards Institute, Wayne, PA (2009).

[25] E. Goldman, L.H. Green, Practical Handbook of Microbiology, 2nd Edn. (2009), 37-39, CRC Press, Taylor & Francis Group, New York.

[26] A.W. Bauer, W.M. Kirby, J.C. Sheris, M. Turck. *Am. J. Clin. Pathol.*, **45**, 493 (1966).

[27] M. Pooyan, A. Ghaffari, M. Behzad, H. Amiri Rudbari, G. Bruno. *J. Coord. Chem.*, **66**, 4255 (2013).

[28] A. Ghaffari, M. Behzad, M. Pooyan, H. Amiri Rudbari, G. Bruno. *J. Mol. Struct.*, **1063**, 1 (2014).

[29] Z. Abbasi, M. Behzad, A. Ghaffari, H. Amiri Rudbari, G. Bruno. *Inorg. Chim. Acta*, **414**, 78 (2014).

[30] V. Selvarani, B. Annaraj, M.A. Neelakantan, S. Sundaramoorthy, D. Velmurugan. *Polyhedron*, **54**, 74 (2013).

[31] G. Grivani, S. Husseinzadeh Baghan, M. Vakili, A. Dehno Khalaji, V. Tahmasebi, V. Eigner, M. Dušek. *J. Mol. Struct.*, **1082**, 91 (2015).

[32] Q.P. Qin, Y.L. Li, Y.C. Liu, Z.F. Chen. *Inorg. Chim. Acta*, **421**, 260 (2014).

[33] M. Rajasekar, S. Sreedaran, R. Prabu, V. Narayanan, R. Jegadeesh, N. Raaman, A. Kalilur Rahiman. *J. Coord. Chem.*, **63**, 136 (2010).

[34] A. Nuri Kursunlu, E. Guler, F. Sevgi, B. Ozkalp. *J. Mol. Struct.*, **1048**, 476 (2013).

[35] P.K. Pal, A. Banerjee, R. Bhadra, A.D. Jana, G.K. Patra. *J. Coord. Chem.*, **67**, 3107 (2014).

[36] S. Sreedaran, K. Shanmuga Bharathi, A. Kalilur Rahiman, K. Rajesh, G. Nirmala, L. Jagadish, V. Kaviyarasan, V. Narayanan. *Polyhedron*, **27**, 1867 (2008).

[37] M. Kalita, P. Gogoi, P. Barman, B, Sarma. *J. Coord. Chem.*, **67**, 2445 (2014).

[38] A. Jayamani, N. Sengottuvelan, G. Chakkaravarthi. *Polyhedron*, **81**, 764 (2014).

[39] C.-F. Jiang, F.-P. Liang, Y. Li, X.-J. Wang, Z.-L. Chen, H.-D. Bian. *J. Mol. Struct.*, **842**, 109 (2007).

[40] P. Knopp, K. Weighardt, B. Nuber, J. Weiss, W.S. Sheldrick. *Inorg. Chem.*, **29**, 363 (2009).

[41] N. Dharmaraj, P. Viswanathamurthi, K. Natarajan. *Transition Met. Chem.*, **26**, 105 (2001).

Table 1. Crystallographic data for CuL^2 and CuL^3.

Crystal data	CuL^2	CuL^3
Formula	$C_{19}H_{16}Br_2CuN_4O_6$	$C_{26}H_{24}Br_2CuN_6O_8$
Formula weight	619.72	771.86
Crystal system	Monoclinic	Triclinic
Space group	C_2/c	P-1
T (K)	298(2)	293(2)
λ (Å)	0.71073	0.71073
Unit cell dimensions (Å, °)		
a (Å)	7.5373(9)	10.730(2)
b (Å)	16.093(2)	11.395(2)
c (Å)	17.635(2)	12.547(3)
α (°)	90.00	78.74(3)
β (°)	98.833	85.36(3)
γ (°)	90.00	84.66(3)
Volume ($Å^3$), Z	2113.7(5), 4	1494.9(5), 2
Calculated density (Mg m^{-3})	1.947	1.715
Absorption coefficient (mm^{-1})	4.860	3.461
F(000)	1220	770
θ range for data collection (°)	2.79 to 27.00	1.83 to 25.00
Limiting indices	-9≤h≤9	-12≤h≤12
	-20≤k≤20	-13≤k≤13
	-22≤l≤22	-14≤l≤14
Data / restraints / parameters	2313 / 0 / 147	4971 / 0 / 370
Total reflections	21213	9797
Unique reflections (R_{int})	2313 [$R_{(int)}$ = 0.0408]	4971[$R_{(int)}$ = 0.0481]
Completeness	99.9 %	94.2 %
Refinement method	Full-matrix least squares on F^2	Full-matrix least squares on F^2
Goodness-of-fit on F^2	1.040	1.108
Final R index [I > 2σ(I)]	R_1 = 0.035, wR_2 = 0.0831	R_1 = 0.035, wR_2 = 0.0831
R index [all data]	R_1 = 0.0434, wR_2 = 0.088	R_1 = 0.0434, wR_2 = 0.088
Largest diff. peak and hole (e $Å^{-3}$)	0.518 and -0.638	0.741 and -0.960

Table 2. Selected bond lengths and angles around copper for CuL^2 and CuL^3.

CuL^2		CuL^3	
Bond lengths (Å)		Bond lengths (Å)	
Cu(1)-O(1)	1.907(2)	Cu(1)-O(3)	1.912 (4)
Cu(1)-O(1')	1.907(2)	Cu(1)-O(5)	1.923 (4)
Cu(1)-N(1)	1.955(3)	Cu(1)-N(4)	1.950 (4)
Cu(1)-N(1')	1.955(3)	Cu(1)-N(5)	1.959 (4)
Bond angles (°)		Bond angles (°)	
O(1)-Cu(1)-O(1')	90.80(13)	O(3)-Cu(1)-O(5)	89.27(15)
O(1)-Cu(1)-N(1)	92.59(10)	O(3)-Cu(1)-N(4)	171.45(17)
O(1)-Cu(1)-N(1')	160.32(12)	O(3)-Cu(1)-N(5)	93.39(16)
O(1')-Cu(1)-N(1')	92.59(10)	O(5)-Cu(1)-N(4)	93.53(16)
O(1')-Cu(1)-N(1)	160.32(12)	O(5)-Cu(1)-N(5)	177.17(16)
N(1)-Cu(1)-N(1')	90.71(15)	N(4)-Cu(1)-N(5)	83.70(17)

Table 3. Redox potential data for 10^{-3} mol L^{-1} solutions of CuL^{x} (x = 1-4) complexes in DMSO solutions containing 0.1 mol L^{-1} TOAB and scan rate 100 mV s^{-1}. Data are in volts.

Complex	$Ep_a(1)$	$Ep_c(1)$	ΔE	E^0
CuL^1	-1.49	-1.57	0.16	-1.49
CuL^2	-1.09	-1.20	0.11	-1.15
CuL^3	-1.41	-1.66	0.18	-1.50
CuL^4	-1.48	-1.67	0.19	-1.57

Table 4. MIC and MBC values (μg mL^{-1}) for the CuL^{1-4} complexes against the studied bacteria.

	CuL^1		CuL^2		CuL^3		CuL^4		Kanamycin	
	MBC	MIC	MBC	MIC	MBC	MIC	MBC	MIC	MBC	MIC
E.coli	625	575	575	525	750	625	1250	1000	3.8	4
S.typhi	500	425	425	375	500	475	750	525	3.2	3.3
S.aureus	425	425	425	325	750	750	750	575	3.0	3.2
B.subtilis	525	475	575	450	750	675	1125	1125	3.6	4.0

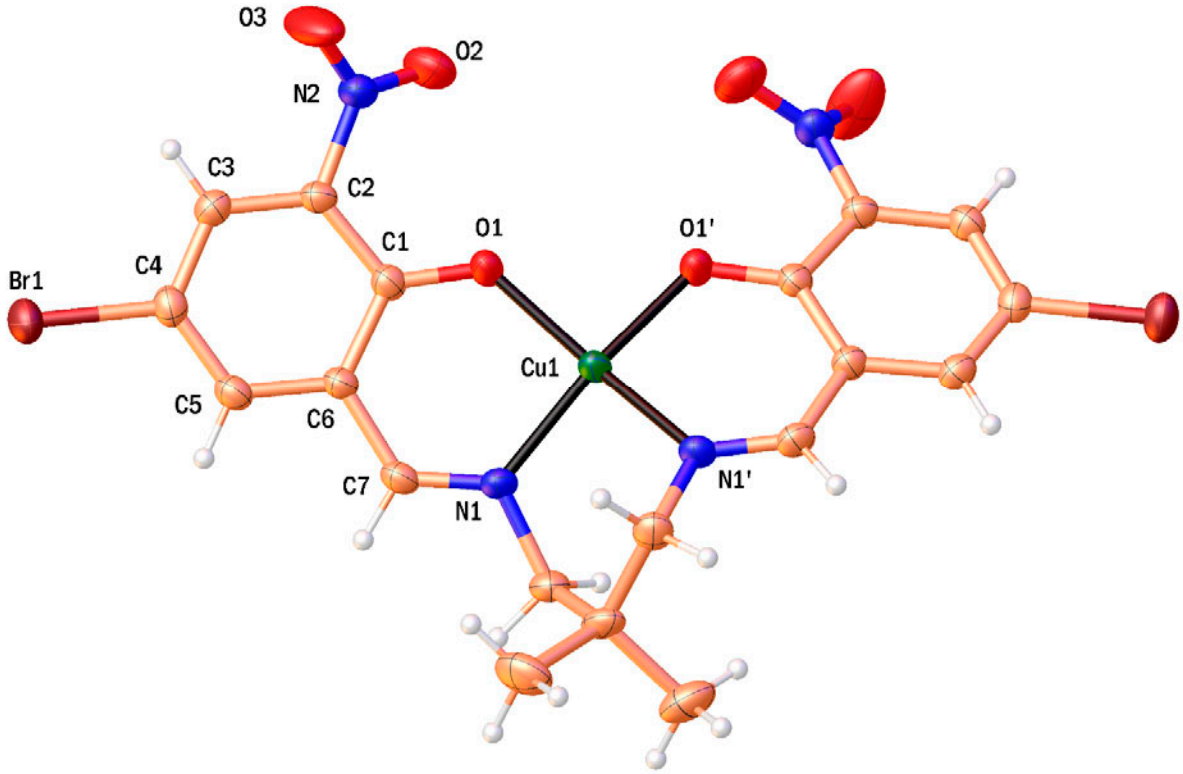

Figure 1. ORTEP representation of CuL^2 with common atom numbering scheme. Displacement ellipsoids are drawn at the 50% probability level and hydrogens are shown as small spheres of arbitrary radii.

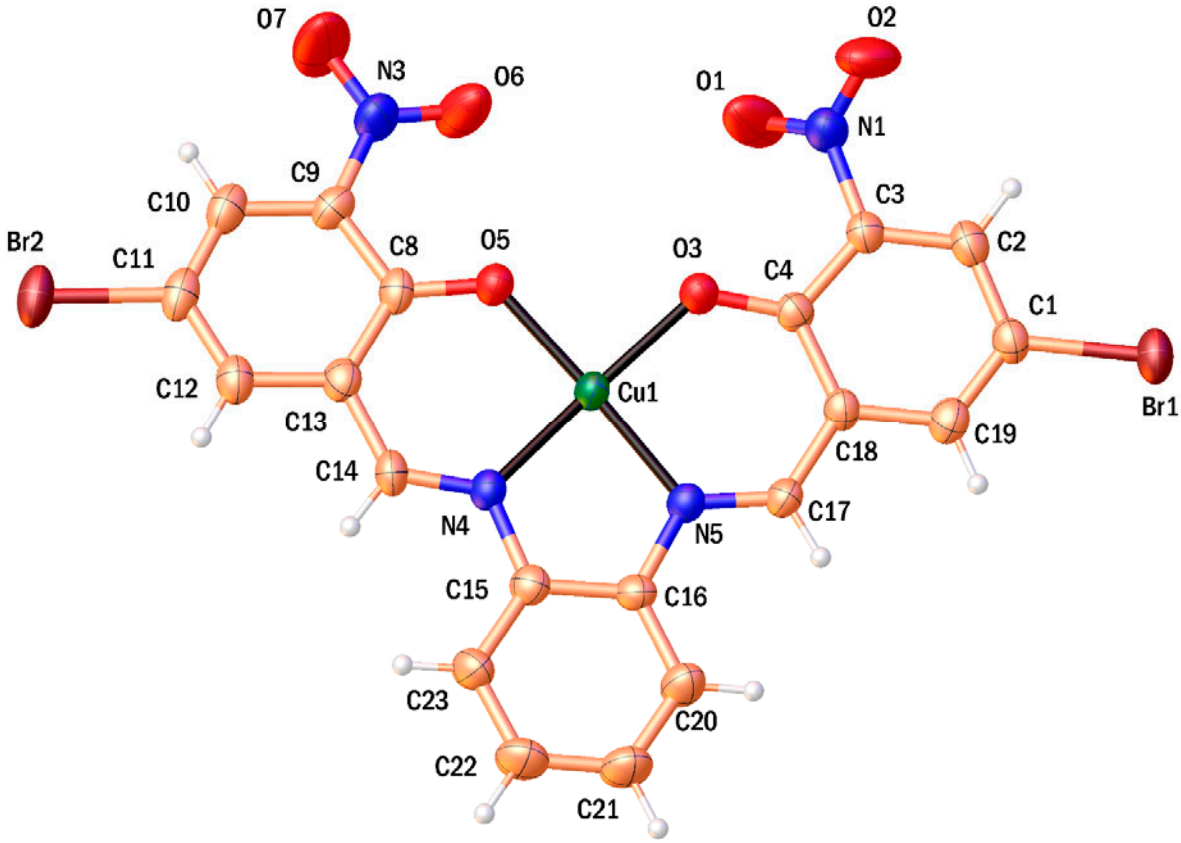

Figure 2. ORTEP representation of CuL^3 with common atom numbering scheme. Displacement ellipsoids are drawn at the 50% probability level and hydrogens are shown as small spheres of arbitrary radii. Uncoordinated solvents of crystallization (two DMF molecules) are omitted for clarity.

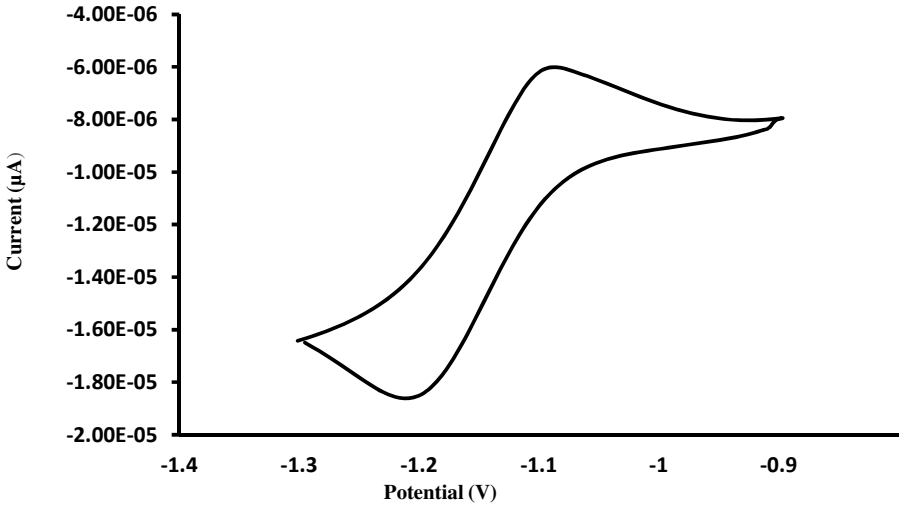

Figure 3. Cyclic voltammogram of CuL^2.

Graphical abstract